nature plants

ARTICLES

https://doi.org/10.1038/s41477-021-00953-7

Check for updates

CRISPR–Act3.0 for highly efficient multiplexed gene activation in plants

Changtian Pan[1], Xincheng Wu[1], Kasey Markel[2], Aimee A. Malzahn[1], Neil Kundagrami[1], Simon Sretenovic[1], Yingxiao Zhang[1], Yanhao Cheng[1], Patrick M. Shih[2,3,4,5,6] and Yiping Qi[1,7] ✉

RNA-guided CRISPR activation (CRISPRa) systems have been developed in plants. However, the simultaneous activation of multiple genes remains challenging. Here, we develop a highly robust CRISPRa system working in rice, *Arabidopsis* and tomato, CRISPR–Act3.0, through systematically exploring different effector recruitment strategies and various transcription activators based on deactivated *Streptococcus pyogenes* Cas9 (dSpCas9). The CRISPR–Act3.0 system results in fourfold to sixfold higher activation than the state-of-the-art CRISPRa systems. We further develop a tRNA–gR2.0 (single guide RNA 2.0) expression system enabling CRISPR–Act3.0-based robust activation of up to seven genes for metabolic engineering in rice. In addition, CRISPR–Act3.0 allows the simultaneous modification of multiple traits in *Arabidopsis*, which are stably transmitted to the T3 generations. On the basis of CRISPR–Act3.0, we elucidate guide RNA targeting rules for effective transcriptional activation. To target T-rich protospacer adjacent motifs (PAMs), we transfer this activation strategy to CRISPR–dCas12b and further improve the dAaCas12b-based CRISPRa system. Moreover, we develop a potent near-PAM-less CRISPR–Act3.0 system on the basis of the SpRY dCas9 variant, which outperforms the dCas9–NG system in both activation potency and targeting scope. Altogether, our study has substantially improved the CRISPRa technology in plants and provided plant researchers a powerful toolbox for efficient gene activation in foundational and translational research.

Sequence-specific nucleases such as ZFNs, TALENs and CRISPR–Cas systems have greatly accelerated plant research and breeding[1–4]. While these tools are widely used for generating loss-of-function mutants, plant researchers still largely rely on the conventional gene overexpression approach for gain-of-function analysis. Under this approach, genomic DNA or cDNA for the gene of interest must be cloned under a strong RNA Polymerase II (Pol II) promoter. Furthermore, the molecular cloning process results in the overexpression of large genes or large numbers of genes being laborious. CRISPR activation (CRISPRa), based on deactivated Cas (dCas) proteins coupled with activator domains, was first demonstrated in human cells[5,6] and provides a promising alternative to the conventional gene overexpression approach in plants[7,8]. Theoretically, CRISPRa could enable the specific activation of any target gene in the genome due to its RNA-guided nature. In addition, CRISPRa is even more advantageous over the conventional overexpression system if multiple genes are involved.

The first-generation CRISPRa system in plants was based on dCas9–VP64 (refs. [9,10]). To boost the activation level of CRISPRa, several groups have recently generated three second-generation CRISPRa systems—namely, dCas9–SunTag[11,12], dCas9–TV[13,14] and dCasEV2.1 (refs. [15,16]). For the dCas9–SunTag system, dCas9 was fused to a tandem array of GCN4 peptides that could recruit the VP64 transcriptional activator[11,12]. While dCas9–TV relied on the fusion of dCas9 with six copies of the transcription activator-like effector (TALE) TAL Activation Domain (TAD) motif coupled with VP128 (6xTAL–VP128 (TV))[13], dCasEV2.1 employed a gRNA2.1 scaffold with anchoring sites for VPR (VP64–p65–Rta) transcriptional activator[16]. These three second-generation CRISPRa systems conferred stronger transcriptional activation than dCas9–VP64. However, these systems were tested in different plant species or with different genes and expression systems, making it unclear which system is the most potent in plants. Our previous study showed that CRISPR–Act2.0, another second-generation CRISPRa system, yielded stronger transcriptional activation than dCas9–VP64 in plants but was less potent than mTALE–Act, a gene activation system based on the TALE, albeit with both using VP64 as the activator[17]. This suggests room for further improvement of CRISPR–Act2.0.

In this study, we developed a third-generation CRISPRa system, CRISPR–Act3.0, with much higher activation potency than any of the various second-generation CRISPRa systems in rice. With CRISPR–Act3.0, we further developed highly potent multiplexed gene activation systems, elucidated design rules for effective target gene activation and demonstrated the simultaneous activation of many enzyme-encoding genes in the β-carotene biosynthesis pathway and the proanthocyanidin biosynthesis pathway in rice as well as multigene activation in *Arabidopsis*. Importantly, we adapted this activation strategy to CRISPR–Cas12b and a near-PAM-less SpCas9 variant, SpRY, which greatly expands the targeting scope for gene activation. We envision that such an improved CRISPRa toolbox would greatly aid functional genomics research as well as multigene activation applications required in plant metabolic engineering and synthetic biology.

Results

Development of the CRISPR–Act3.0 system. Our previous CRISPR–Act2.0 system used an engineered gRNA2.0 (gR2.0) scaffold that contains two MS2 RNA aptamers for recruiting the

[1]Department of Plant Science and Landscape Architecture, University of Maryland, College Park, MD, USA. [2]Department of Plant Biology, University of California, Davis, CA, USA. [3]Environmental Genomics and Systems Biology Division, Lawrence Berkeley National Laboratory, Berkeley, CA, USA. [4]Feedstocks Division, Joint BioEnergy Institute, Emeryville, CA, USA. [5]Department of Plant and Microbial Biology, University of California, Berkeley, CA, USA. [6]Innovative Genomics Institute, University of California, Berkeley, CA, USA. [7]Institute for Bioscience and Biotechnology Research, University of Maryland, Rockville, MD, USA. ✉e-mail: yiping@umd.edu

activator VP64 through the MS2–MCP interaction[17]. We reasoned that if we installed more MS2 aptamers into the single guide RNA (sgRNA) scaffold, the system could recruit more VP64, which might lead to improved gene activation. We adopted sgRNA scaffolds containing 8 unique MS2 RNA aptamers (gR8xMS2)[18] and 16 unique MS2 RNA aptamers (gR16xMS2)[19], as both scaffolds were previously demonstrated to recruit many copies of fluorescent proteins for live cell imaging of mammalian cells (Supplementary Fig. 1a). We compared these two new VP64-recruiting systems coupled with CRISPR–Act2.0 for gene activation in rice protoplasts. Two independent genes, *OsGW7* and *OsER1*, were targeted for activation[13]. We also compared OsU3 (rice U3, a Pol III promoter) and ZmUbi (maize ubiquitin 1, a Pol II promoter) for expressing the sgRNAs. To guide proper sgRNA maturation in the ZmUbi promoter system, we used the tRNA processing system[20]. To our surprise, neither gR8xMS2 nor gR16xMS2 showed higher gene activation levels than the CRISPR–Act2.0 system, on the basis of quantitative PCR with reverse transcription (RT–qPCR) analysis (Supplementary Fig. 1b,c). We found that the guide RNA level of gR16xMS2 was much lower than those of gR2.0 and gR8xMS2 with either promoter (Supplementary Fig. 1d), indicating that the instability of gR16xMS2 might be the bottleneck for its activation efficiency[18]. In addition, compared with OsU3, ZmUbi produced higher guide RNA levels (Supplementary Fig. 1d). To recruit more VP64 with these three sgRNA scaffolds, we modified a split GFP system[21]. In our system, a deactivated plant codon-optimized Cas9 (dpcoCas9)[22] is fused to seven tandemly arrayed GFP11 peptides and co-expressed with a GFP1-10–VP64 fusion protein (Supplementary Fig. 2a). Upon GFP reconstitution, a single dCas9/sgRNA complex is expected to recruit many VP64 to a target site. Testing this strategy in rice protoplasts, however, did not yield gene activation for either *OsGW7* or *OsER1* (Supplementary Fig. 2b,c).

These earlier attempts suggested that some strategies that successfully recruit fluorescent proteins for DNA imaging do not result in gene activation through the recruitment of transcription activators such as VP64. This could be due to the complex process of gene activation, as it requires further recruitment of transcription machinery based on the activators. The SunTag system has been previously established for gene activation in both human cells[11] and plants[10]. In the SunTag system, the tandemly arrayed GCN4 epitopes are directly fused to the C-terminus dCas9 to recruit VP64 through a single-chain antibody, scFv[11,12]. We hypothesized that coupling the SunTag system with the MS2–MCP interaction would recruit more VP64 (Fig. 1a). To test this strategy, we compared both gR2.0 (refs. [17,23]) and gR8xMS2 (ref. [18]) scaffolds with two different lengths of SunTag (four or ten repeats of GCN4 epitopes, 4xGCN4 and 10xGCN4). We assessed these configurations in rice protoplasts by activating *OsGW7* and *OsER1*. With the gR2.0 scaffold, both the 4xGCN4 and 10xGCN4 tags resulted in pronounced gene activation at both targets, which was tenfold higher than the level induced by the CRISPR–Act2.0 system (Fig. 1b). The gR8xMS2 scaffold also generated significant activation, though less potent than the gR2.0 scaffold (Fig. 1b). These results reinforced the notion that more MS2 aptamers did not necessarily translate into higher gene activation.

Encouraged by the success in combining the SunTag system with the MS2 system, we next developed two new activators: two repeats of TAD (2xTAD) and 2xTAD coupled with a VP64 (2xTAD–VP64). We compared these activators with the previously reported activators VP64, TV[13] and VPR[15] to test this platform by targeting *OsER1* in rice protoplasts (Fig. 1c). With the 4xGCN4 SunTag, the systems with 2xTAD and 2xTAD–VP64 activators showed the highest gene activation (>100-fold) (Fig. 1c). With the 10xGCN4 SunTag, the 2xTAD activator system resulted in the highest activation of the target gene, ~250-fold (Fig. 1c). This result pointed to a highly efficient gene activation system that combines dCas9–VP64, gR2.0 scaffold, 10xGCN4 SunTag and the newly developed 2xTAD activator. We consider this new system as a third-generation CRISPRa system and named it CRISPR–Act3.0. To benchmark CRISPR–Act3.0, we compared it with three additional second-generation CRISPRa systems previously developed by other research groups, including dCas9–SunTag[11,12], dCas9–TV[13] and dCasEV2.1 (ref. [16]) (Fig. 1d). To ensure close comparison, the same vector backbones and promoters were used. By targeting the same two genes (*OsGW7* and *OsER1*) with the same sgRNAs, we found that dCas9–TV resulted in ~40-fold activation of both genes, an activation level comparable to the previous report on using dCas9–TV to activate these genes[13]. With this level of gene activation, the dCas9–TV system outperformed the dCas9–SunTag and dCasEV2.1 systems (Fig. 1d). Strikingly, CRISPR–Act3.0 generated activation four to six times stronger than dCas9–TV at both target genes, with over 250-fold for *OsGW7* and over 100-fold for *OsER1*, regardless of the promoter (OsU3 or ZmUbi) used to drive the single sgRNA expression (Fig. 1d). To further benchmark CRISPR–Act3.0, we targeted a third gene in rice, *OsBBM1*, whose overexpression in egg cells was recently shown to help the asexual propagation of rice seeds[24]. To rule out the possibility that the superior performance of CRISPR–Act3.0 is position-dependent, we targeted three distinct positions in the *OsBBM1* promoter (Supplementary Fig. 3a). We found that CRISPR–Act3.0 resulted in significantly higher activation efficiency at two target sites and considerably improved activation at one target site compared with the other three activation systems: 6-fold to 24-fold higher at two target sites and 1.3-fold to 2.9-fold higher at the third site (Supplementary Fig. 3b). Since both the gR2.0 and gRNA2.1 scaffolds contain two MS2 stem loops (albeit at different positions)[16,17,23], we compared them and found that gRNA2.1 worked poorly in the CRISPR–Act3.0 configuration for gene activation compared with gRNA2.0 (Supplementary Fig. 3c). Together, our work established gR2.0-based CRISPR–Act3.0 as a third-generation CRISPRa system that is much more potent than earlier systems based on our assays in rice protoplasts.

Fig. 1 | Development of the CRISPR–Act3.0 system. a, Schematic illustration of the CRISPR–Act3.0 strategy. The dSpCas9 is fused with a VP64, and the coupled gR2.0 contains two MS2 RNA aptamers (in pink) for recruiting the MS2 bacteriophage coat protein (MCP), which is fused to the SunTag. The single-chain variable fragment (scFv) of GCN4 antibody is fused to a super folder green fluorescent protein (sfGFP), which serves as a linker for the scFv and activator fusion. **b**, Comparison of different sgRNA scaffolds and 4xGCN4 or 10xGCN4 epitopes for gene activation. **c**, Comparison of different activators for gene activation. The different letters indicate significantly different mean values at $P < 0.05$ (one-way analysis of variance (ANOVA) with post-hoc Tukey test). **d**, Comparison between CRISPR–Act3.0 and three other potent second-generation CRISPR-activation systems. In Act3.0–ZmUbi, a Pol II promoter, ZmUbi, was used for sgRNA expression, coupled with the tRNA processing system. The other systems used OsU3 for sgRNA expression. The dashed horizontal line indicates the highest gene activation level from the second-generation CRISPRa systems compared. **e**, Activation of an mCherry gene by an sgRNA. Tested promoters with intact 5′ UTR sequences are fused to the mCherry coding sequence. **f**, Detection of mCherry signals without (−Act3.0) and with the CRISPR–Act3.0 activation system (+Act3.0) in rice cells. The mCherry signals were detected using a fluorescence microscope 24 hours after rice protoplast transformation. **g**, Statistical analysis of mCherry-positive cells with and without the CRISPR–Act3.0 activation system. All data are presented as the mean ± s.d. ($n = 5$ independent scopes). $^{**}P < 0.01$, two-tailed Student's *t*-tests. For the RT–qPCR assays (**b**–**d**), T-DNA vectors without sgRNAs served as the negative control (CTRL). *OsTubulin* is used as the endogenous control gene. All data are presented as the mean ± s.d. ($n = 3$ independent experiments). $^{*}P < 0.05$, $^{**}P < 0.01$, two-tailed Student's *t*-tests.

We next sought to visualize the CRISPR–Act3.0-mediated activation by using an mCherry reporter system. Two randomly selected promoters, Pro*OsTPR-like* and Pro*OsCCR1*, were used to drive mCherry expression, generating two corresponding mCherry reporter constructs (Fig. 1e). As a positive control, mCherry was driven by the strong ZmUbi promoter. Each promoter except the

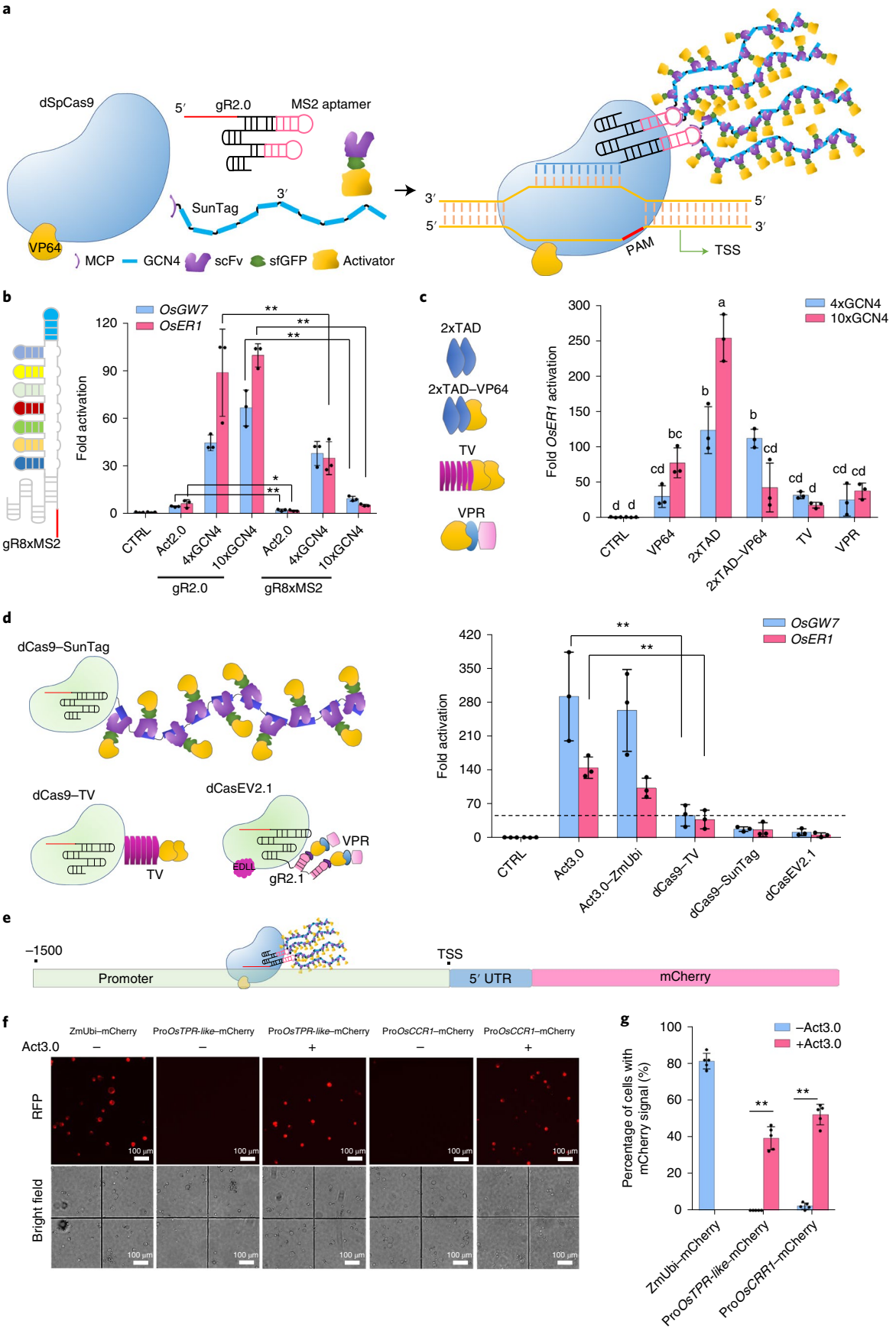

positive control was targeted by one sgRNA to evaluate the robustness of CRISPR–Act3.0. Notably, the co-transformation of rice protoplasts with the CRISPR–Act3.0 construct and the reporter construct in both cases resulted in red fluorescent cells indicative of strong mCherry expression; in contrast, such signals were absent without the use of either sgRNA (Fig. 1f). Further quantification showed that 80% of cells were mCherry-positive from the ZmUbi::mCherry positive control. About 40% and 50% of cells co-transformed with the CRISPR–Act3.0 and the mCherry report constructs were mCherry-positive, respectively (Fig. 1g), suggesting that CRISPR–Act3.0-induced activation potency can be indicated by fluorescence intensity. In addition, CRISPR–Act3.0 activated the transcription of the endogenous genes *OsTPR-like* and *OsCCR1* in rice with ~60-fold and ~20-fold activation, respectively (Supplementary Fig. 3d). Taken together, these data demonstrated robust gene activation by CRISPR–Act3.0 with a single sgRNA.

Multiplexed gene activation in rice. The tRNA-based processing system is highly compact and efficient for multiplexing sgRNAs in plants[20,25], yeast[26], *Drosophila*[27] and human cells[28]. To enable efficient multiplexed gene activation in rice, we developed a streamlined cloning system for one-step assembly of up to six tRNA–gRNA2.0 cassettes (Fig. 2a) or U3–gRNA2.0 cassettes (based on a conventional gRNA2.0 system) (Supplementary Fig. 4). One Pol II promoter, ZmUbi, was employed to drive the expression of all tRNA–gRNA2.0 cassettes, and in contrast, one U3 promoter was used for each individual U3–gRNA2.0 cassette expression (Fig. 2a and Supplementary Fig. 4). To compare this multiplexed tRNA–gRNA2.0 (M-tRNA) system with the conventional multiplexed U3–gRNA2.0 (M-U3) system where sgRNAs were expressed in independent transcription units[17], we targeted three genes (*OsGW7*, *OsER1* and *OsPXL2*) in rice for simultaneous activation (Fig. 2b). These two multiplex constructs, M-tRNA and M-OsU3, were compared with individual gene activation constructs (I-OsU3). At the three target genes, M-tRNA resulted in comparable levels of fold activation to I-OsU3 and better activation than M-OsU3 for multiplexed gene activation (Fig. 2b). We next compared single sgRNA and multiplexed sgRNAs for gene activation at two independent loci. At *OsGW7*, multiplexing three gRNAs generated higher gene activation than single gRNAs alone (Supplementary Fig. 5a). At *OsTPR-like*, multiplexing three sgRNAs generated a similar level of gene activation to the best-performing single sgRNA (Supplementary Fig. 5b). These data suggest that multiplexing a few sgRNAs represents a safe strategy to achieve robust gene activation, consistent with earlier observations in plants[16,17,29].

However, we also found that highly efficient singular sgRNAs could be identified using a protoplast-based prescreen process. In most cases, the activation level with a single sgRNA would be strong enough for the target gene, which reserves much room for multiplexing many genes, as only one sgRNA is used for one gene. To demonstrate this one-sgRNA-for-one-gene strategy, we sought to apply CRISPR–Act3.0 to target metabolic pathway genes with the M-tRNA system. In the first demonstration, we targeted seven enzyme-encoding genes in the β-carotene pathway in rice. For each gene, three to four sgRNAs were tested in rice protoplasts in the prescreen step. The prescreen data in rice protoplasts showed that four of seven genes could be activated tenfold or higher (Supplementary Fig. 6a). We then picked the best-performing sgRNAs for each target gene and assembled them into one M-Act3.0 vector based on the M-tRNA system according to a higher-order assembly method[30]. Gene activation of up to 20-fold was found for all seven target genes using the M-Act3.0 vector in rice protoplasts (Supplementary Fig. 6b). In the second demonstration, we targeted six enzyme-encoding genes in the proanthocyanidin pathway in the *indica* rice variety Kasalath (Supplementary Fig. 7a). For each gene, three to six sgRNAs were tested in rice protoplasts in the prescreen step, and in all cases except *OsCHI*, at least one sgRNA could be identified with >30-fold gene activation levels (Supplementary Fig. 7b). Stacking the six high-activity sgRNAs with the M-tRNA system (Fig. 2a) led to pronounced simultaneous gene activation for five out of six target genes (Fig. 2c). We also targeted three regulatory genes (*OsRc*, *OsTTG1* and *OsTT2*) in the proanthocyanidin pathway[31] (Supplementary Fig. 8a). Two sgRNAs were employed for each target gene. These regulatory genes were individually activated by M-Act3.0, and two of them were activated by 40-fold simultaneously with the M-tRNA system (Supplementary Fig. 8b,c).

Furthermore, we used *Agrobacterium*-mediated transformation to introduce an M-Act3.0 vector targeting the six enzyme-encoding genes in the proanthocyanidin pathway and the no-sgRNA control vector into the *indica* rice variety Kasalath. The M-Act3.0 system resulted in a similar activation pattern for all target genes except *OsLAR* in both rice protoplast cells and transgenic callus (Fig. 2c,d and Supplementary Fig. 9a), and four out of six target genes were activated by 5-fold to 140-fold (Fig. 2d). However, only *OsF3H* had a significant activation of ~20-fold in M-Act3.0 transgenic seedlings (leaves) (Fig. 2e and Supplementary Fig. 9b), and the other five target genes could only be activated twofold to eightfold (Fig. 2e). In addition, no difference in phenotype in both callus and seedlings was observed between the M-Act3.0 and CTRL transgenic lines (data not shown). Taken together, we have developed a multiplexed CRISPR–Act3.0 system and demonstrated its use for the simultaneous activation of many genes in the agriculturally relevant crop, rice. Our data also suggest that the potency of CRISPRa is shaped by the endogenous gene regulatory mechanisms, which may vary among genes and pathways.

Fig. 2 | Multiplexed gene activation by CRISPR–Act3.0 in rice. a, Schematic illustrations of assembling sgRNAs for multiplexed gene activation. Multiple sgRNAs are inserted into the BsaI-digested gR2.0 (guide RNA scaffold containing two MS2 RNA aptamers) entry plasmids and then assembled using Golden Gate cloning. The final T-DNA expression vector is constructed by Gateway cloning-mediated assembly of dCas9-activator and tRNA–gR2.0 array cassettes into a destination vector of choice. Two to six sgRNAs are easily assembled on the basis of this strategy. Spectinomycin-R, spectinomycin resistance gene; kanamycin-R, kanamycin resistance gene; RB, right border; LB, left border; Ter, terminator. **b**, Comparison of different multiplexed gene activation strategies based on CRISPR–Act3.0 for simultaneous gene activation. I-OsU3, singular gene activation with individual gR2.0 expression cassettes each driven by an OsU3 promoter. M-tRNA, multiple tRNA-mediated gR2.0 expression cassettes driven by the Pol II promoter ZmUbi. M-OsU3, multiple tandem repeats of independent OsU3-based gR2.0 expression cassettes. T-DNA vectors without sgRNAs served as the negative control. *OsTubulin* is used as the endogenous control gene. All data are presented as the mean ± s.d. ($n = 3$ independent experiments). The different letters indicate significantly different mean values at $P < 0.05$ (one-way ANOVA with post-hoc Tukey test). **c**, Simultaneous activation of multiple enzyme-encoding genes of the proanthocyanidin pathway in rice protoplasts. M-Act3.0, CRISPR–Act3.0-mediated multiplexed gene activation using the M-tRNA system. T-DNA vectors without sgRNAs served as the negative control. *OsTubulin* is used as the endogenous control gene. All data are presented as the mean ± s.d. ($n = 3$ independent experiments). **d**, Expression analysis of proanthocyanidin biosynthetic genes in T0 positive transgenic callus. **e**, Expression analysis of proanthocyanidin biosynthetic genes in T0 positive transgenic seedlings (leaves). Act3.0-M#3, 4 and 8 represent different transgenic callus (**d**) and seedlings (**e**) with CRISPR–Act3.0-mediated multiplexed gene activation using the M-tRNA system. For the RT–qPCR assays (**d**,**e**), T0 lines containing T-DNA vectors without sgRNAs served as the negative control. *OsTubulin* is used as the endogenous control gene. All data are presented as the mean ± s.d. ($n = 3$ technical replicates).

It is worth noting that the final transfer DNA (T-DNA) vector expressing dpcoCas9–Act3.0 and M-tRNA components could cause DNA rearrangements in *Agrobacterium tumefaciens* EHA105 despite the fact that different promoters (ZmUbi, UBQ10 (ubiquitin-10) or a cauliflower mosaic virus 35S) were used to drive the dpcoCas9 expression (Supplementary Fig. 10a–e). However, such DNA rearrangements were found in the combination of dpcoCas9–Act3.0 and M-U3 systems (Supplementary Fig. 10c–e). In contrast, we found that CRISPR–Act3.0 based on dzCas9 (a maize codon-optimized dSpCas9)[9,32] did not cause any DNA rearrangement in the plasmids in *A. tumefaciens* (Supplementary Fig. 10f–h). The dzCas9-based CRISPR–Act3.0 system induced a comparable activation efficiency to the dpcoCas9-based CRISPR–Act3.0 system (Supplementary Fig. 11), consistent with previous reports that both pcoCas9 and zCas9 proteins were efficient for genome editing[33].

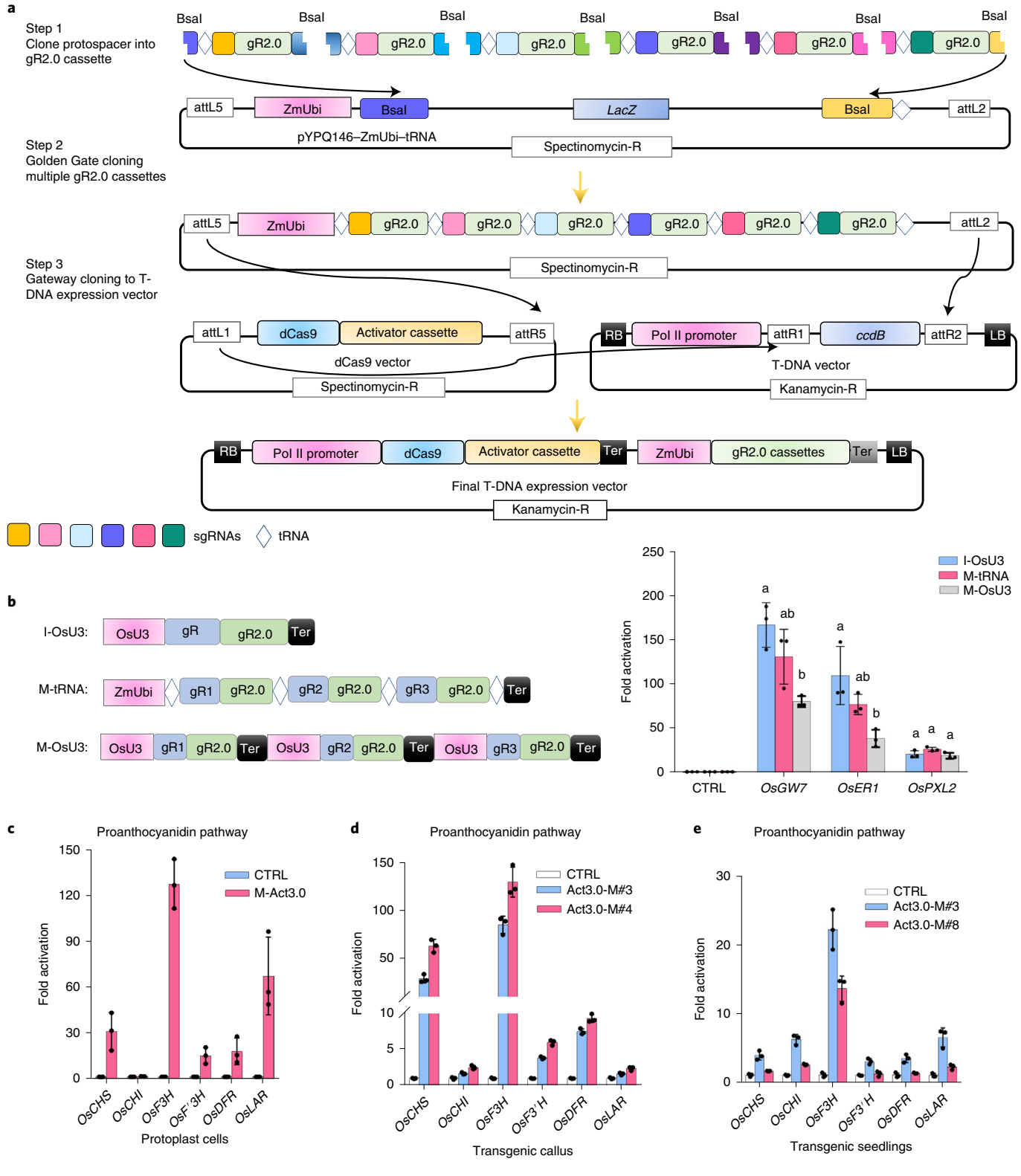

Multiplexed gene activation in dicot plants. To assess CRISPR–Act3.0 in dicot plants, we simultaneously targeted two genes, *AtFT* (regulating flowering)[34] and *AtTCL1* (regulating trichome development)[35], in the model plant *Arabidopsis* using the dpcoCas9-based CRISPR–Act3.0 system. Each gene was targeted with two sgRNAs, and the four corresponding sgRNAs were assembled on the basis of the streamlined cloning system (Fig. 3a and Supplementary Fig. 4). All T1 transgenic plants clearly displayed an early flowering phenotype (Fig. 3b), an anticipated phenotype for robust *AtFT* overexpression[34,36]. The phenotype was further quantified by counting the number of rosette leaves upon flowering. The control plants showed about four times more rosette leaves than the *AtFT* overexpression lines (Fig. 3c). A plant life cycle analysis showed that transgenic plants on average reduced their seed-to-seed life cycle by ~30 days compared with the no-sgRNA transgenic control plants (Fig. 3d). The expression levels of *AtFT* and *AtTCL1* were activated by 130-fold to 240-fold and 3-fold to 8-fold, respectively, in early flowering T1 plants (Fig. 3e). It is worth noting that relatively low levels of gene activation for *AtTCL1* could be due to the lack of prescreening sgRNA activities. We further examined the elevated expression levels of *AtFT* and *AtTCL1* as well as the resulting early flowering and reduced trichome development in the T2 and T3 generations. A high percentage of the early flowering phenotype (~85%) was identified in both T2 and T3 populations of Act3.0-#4 and Act3.0-#10 lines (Fig. 3e,f). In addition, the numbers of trichomes per leaf of Act3.0-#4 and Act3.0-#10 lines were significantly decreased in both T2 and T3 populations (Fig. 3g). Consistent with the phenotypes, similar levels of gene activation for both *AtFT* (80-fold to 500-fold) and *AtTCL1* (3-fold to 20-fold) were found in both T2 and T3 populations (Fig. 3e,f). These results suggest that CRISPR–Act3.0 is a robust gene activation tool in a dicot plant species and that multiplexed CRISPR–Act3.0-mediated modifications of phenotypes can be stably transmitted across multiple generations. Translation of the success in CRISPR–Act3.0-mediated endogenous *FT* activation in *Arabidopsis* into crops would have transformative impacts in accelerating crop breeding.

Since zCas9 resulted high-efficiency genome editing in dicot plants such as *Arabidopsis*[32] and carrot[37], the dzCas9–Act3.0 system presumably should work well for gene activation in dicot plants. We tested dzCas9–Act3.0 in tomato. Four different sgRNAs (gR1 to gR4) were designed to target the promoter of the *SFT* gene in tomato. On the basis of a protoplast assay, gR1 and gR2 each resulted in 240-fold transcription activation, while gR3 and gR4 generated ~30-fold and 20-fold transcription activation, respectively (Fig. 3h). The data suggest that dzCas9–Act3.0 is very potent in tomato and that the levels of target gene activation are determined by the sgRNAs and their target positions.

Design rules for efficient sgRNAs in CRISPR–Act3.0 applications. Our work here, along with earlier studies in plants, has shown that gene activation efficiency varies among different sgRNAs for the same target gene[9,11,13,16,17,29]. When designing sgRNAs, we had already focused on the most effective promoter region, which is 0 base pairs (bp) to −250 bp from the transcription start site (TSS), according to earlier studies in humans[5,6,12,15,23]. To provide further guidance in sgRNA design for implementing CRISPR–Act3.0 in plants, we investigated the protoplast-based gene activation data from 56 sgRNAs targeting the −3-bp to −261-bp region from the TSS of 16 genes in rice. We found that most sgRNAs were effective in the 0-bp to −200-bp region from the TSS (Fig. 4a). Interestingly, sgRNAs targeting the noncoding strand of DNA were overrepresented (13/19; sgRNAs targeting the noncoding strand / total sgRNAs, $P < 0.05$, two-tailed binomial probability test) among these active sgRNAs with the threshold of 20-fold activation (Fig. 4a), suggesting that sgRNAs targeting the noncoding-strand DNA are preferred to achieve higher activation activity. Further analyses showed that sgRNAs with GC content between 45% and 60% resulted in higher frequencies of robust gene activation (the average activation was 34.8-fold within the optimum range and 12.4-fold outside the optimum range, $P < 0.05$, Kruskal–Wallis test) (Fig. 4b). This trend matches prior reports that sgRNAs with extreme GC contents are less active for gene editing[38]. We note that these design guidelines, although useful for the initial implementation of CRISPR–Act3.0, require further corroboration and investigation with larger datasets, ideally from different plant species.

Expanding the targeting scope of CRISPR–Act3.0. The narrow high-activity targeting window, high-activity GC contents and preference for targeting noncoding-strand DNA would collectively limit the sgRNA choice in designing and implementing CRISPR–Act3.0 in plants. It is also important to avoid targeting cis-regulatory elements so that the binding of the CRISPR–Act3.0 components will not interfere with the recruitment of endogenous transcription factors and regulators necessary for transcription. In light of all these issues, it could be challenging to find many potentially good target sites for CRISPR–Act3.0 based on SpCas9, which recognizes NGG protospacer adjacent motifs (PAMs)[39]. The limited target choices when targeting *AtTCL1* in *Arabidopsis* may partly explain the relatively low level of gene activation that we observed for this gene (Fig. 3e). Many promoters in plants are AT rich[40], making them difficult to target with SpCas9. Recently, we developed CRISPRa systems based on dCas12b proteins, which recognize VTTV (V stands for A, C and G) PAMs[41]. The most efficient Cas12b activation system used an Aac.3 sgRNA scaffold that contains one MS2 stem loop[41] (Fig. 5a). We were curious whether we could transfer the SpCas9-based CRISPR–Act3.0 strategy into Cas12b systems. To this end, we adopted and engineered three additional sgRNA scaffolds, including Aa.3.8.3 (ref. [42]), Aac.4 and Aa.3.8.5 (Fig. 5a and Supplementary Fig. 12), which were meant to use one or two MS2 stem loops to

Fig. 3 | Multiplexed gene activation by CRISPR–Act3.0 in dicot plants. a, Schematic of CRISPR–Act3.0-mediated multiplexed gene activation in *Arabidopsis*. *AtFT* and *AtTCL1* are targeted by two sgRNAs each for activation. gR, sgRNA. **b**, Early flowering phenotype in the T1 population of CRISPR–Act3.0 transgenic plants (Act3.0) and CTRL plants. **c**, Number of rosette leaves in the CTRL and the CRISPR–Act3.0 transgenic *Arabidopsis* plants upon flowering. The box plot boundaries represent the 25th and 75th percentiles, the centre lines indicate the medians and the whiskers extend 1.5 times the interquartile range from the 25th and 75th percentiles. Individual data points are represented by dots. All data are presented as the mean ± s.d. ($n = 14$ independent plants). **d**, *AtFT* activation shortens the life cycle of *Arabidopsis*. C, no-sgRNA transgenic control plants; A, CRISPR–Act3.0 transgenic plants; d, days; seeds, the seeds germinate; silique, the first silique is produced; maturing, the siliques become mature. **e**,**f**, Analysis of the early flowering phenotype and target gene expression (*AtFT* and *AtTCL1*) in T2 (**e**) and T3 (**f**) generations. Two independent CRISPR–Act3.0 populations and one CTRL population are shown for each generation. All data are presented as the mean ± s.d. ($n = 3$ technical replicates). *EF-1α* is used as the endogenous control gene. **g**, Trichome density on the first two true leaves of Act3.0 transgenic and CTRL plants in both T2 and T3 generations. Two independent CRISPR–Act3.0 populations and one CTRL population are shown for each generation. All data are presented as the mean ± s.e. ($n = 19$ and 14 individual plants for the T2 and T3 generations, respectively). The different letters indicate significantly different mean values at $P < 0.05$ (one-way ANOVA with post-hoc Tukey test). Scale bars, 0.5 mm. **h**, Determination of the dzCas9–Act3.0-based activation efficiency in tomato protoplasts. Four individual sgRNAs targeting *SFT* were designed and tested. T-DNA vectors without sgRNAs served as the negative control. *SlUbi3* is used as the endogenous control gene. All data are presented as the mean ± s.d. ($n = 3$ independent experiments).

recruit 10xGCN4 and 2xTAD through the MS2–MCP interaction. We targeted *OsGW7* as well as a morphogenic gene, *OsBBM1* (ref. [24]), in rice protoplasts. For both genes, Aac.3, Aa.3.8.3 and Aa.3.8.5 sgRNA scaffolds resulted in twofold higher activation than our previously established dAaCas12b–TV–MS2–VPR activation system[41] (Fig. 5a). Notably, the Aac.4 sgRNA scaffold that contains two MS2 stem loops generated fourfold to fivefold higher activation than the dAaCas12b–TV–MS2–VPR system (Fig. 5a). We have thus engineered an improved CRISPRa system based on AaCas12b and the Aac.4 sgRNA scaffold.

However, we realized that the improved Cas12b activation system was not as strong as the SpCas9-based CRISPR–Act3.0 system. We therefore decided to relax the PAM requirements of SpCas9 in CRISPR–Act3.0. One promising SpCas9 variant is Cas9–NG, which recognizes NG PAMs in human cells[43] and in plants[44–48]. Another promising SpCas9 variant is SpRY, which was recently claimed as

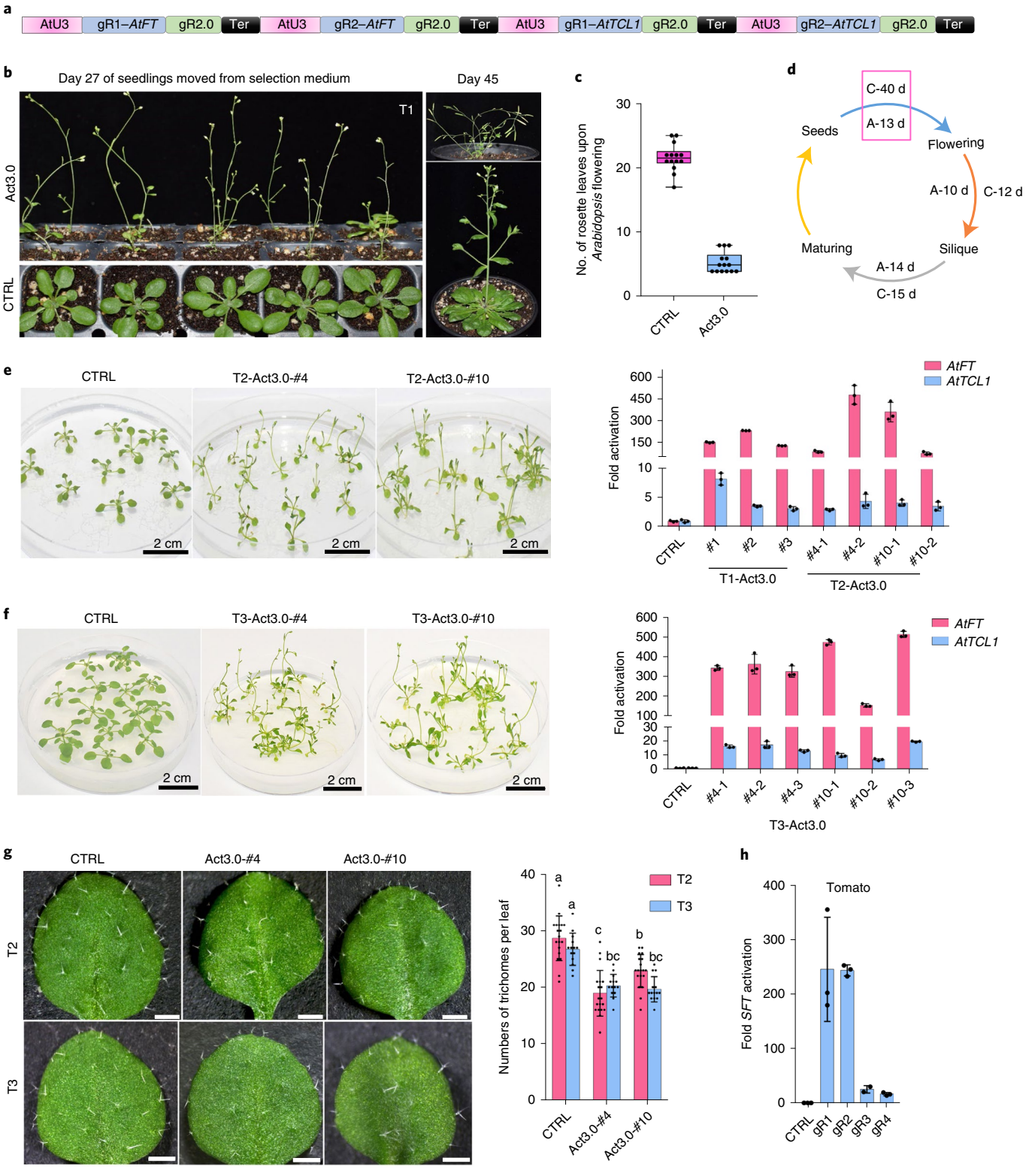

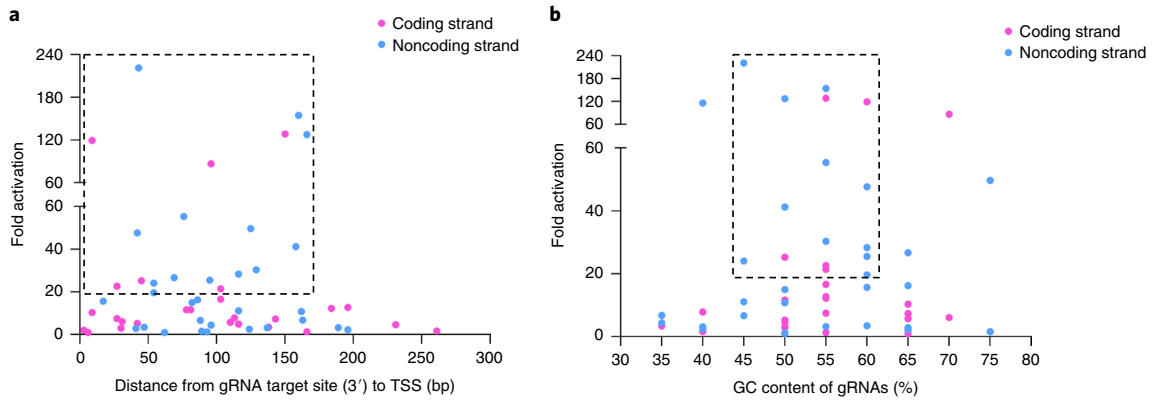

Fig. 4 | Effects of sgRNA position and GC composition on CRISPR–Act3.0-mediated activation in rice. a,**b**, Gene activation levels in rice cells with different sgRNA target site positions (**a**) and GC compositions (**b**). A total of 56 sgRNAs from 16 different genes are analysed with 3 or 4 sgRNAs per gene; each dot indicates one sgRNA. Among these, 26 sgRNAs for 14 different genes target the coding strand, and 30 sgRNAs for 15 different genes target the noncoding strand. A total of 19 sgRNAs (dots) from 12 different genes with more than 20-fold activation are included in the dashed box in **a**. A total of 16 sgRNAs (dots) from 11 different genes with more than 20-fold activation are included in the dashed box in **b**. The pink dots indicate sgRNAs targeting the coding strand; the blue dots indicate sgRNAs targeting the noncoding strand.

near-PAM-less since it can edit NR (R stands for G and A) PAM sites with high efficiency and NY (Y stands for C and T) PAM sites with relatively low efficiency[49]. To compare both SpCas9 variants, we engineered dzCas9–NG–Act3.0 and dSpRY–Act3.0 (based on the same maize codon-optimized Cas9) (Fig. 5b) and compared them with the dzCas9–Act3.0 targeting nearly the same location at four NGN (NGA, NGT, NGC and NGG) PAM sites in the promoter of *OsGW7* (Fig. 5c). Because SpCas9 can target NGA PAMs[50], dzCas9–Act3.0 generated robust activation (>20-fold) as expected at the canonical NGG PAM site and the non-canonical NGA PAM sites (Fig. 5d). Interestingly, we also observed high levels of activation with dzCas9–Act3.0 at the NGC PAM site but not at the NGT PAM site (Fig. 5d). Impressively, dSpRY–Act3.0 resulted in >20-fold target gene activation at all four NGN PAM sites (Fig. 5d). By contrast, dzCas9–NG–Act3.0 generated lower than 20-fold activation at three NGN PAM sites (Fig. 5d). We then compared these systems at a second gene, *OsBBM1*, at four overlapping targeting sites with four NGN (NGA, NGT, NGC and NGG) PAM sites closer to the TSS (Fig. 5e). At this gene, dzCas9–Act3.0 was able to activate transcription only through an NGG PAM-targeting sgRNA (Fig. 5f). By contrast, dSpRY–Act3.0 activated the targets at all four NGN PAM sites (with fold activation ranging from 10 to 200) and outperformed dzCas9–NG–Act3.0 at all these target sites (Fig. 5f). These results demonstrated that dSpRY–Act3.0 targets NGN PAMs more efficiently than dzCas9–NG–Act3.0. However, for targeting NGG PAM sites, dzCas9–Act3.0 induced a higher efficiency than dSpRY–Act3.0. To determine whether dSpRY–Act3.0 could target NAN, NTN and NCN PAMs for gene activation, we picked 12 target sites with NNN PAMs (4 NAN, 4 NTN and 4 NCN) further from the TSS of *OsBBM1*, and these target sites were largely overlapped for close comparisons (Fig. 5e). The data showed that with dSpRY–Act3.0, 11 out of 12 sgRNAs resulted in the activation of *OsBBM1* (Fig. 5g). Together, dSpRY–Act3.0 seems to enable near-PAM-less gene activation in plants, consistent with its near-PAM-less gene editing in human cells[49].

Discussion

In plant functional genomics, a central question is to define the causal relationships between gene expression and phenotypic features in plants. CRISPRa represents a promising approach to streamline and expedite such research by targeting gene activation in plants[8]. To improve the activation potency, targeting flexibility and scalability of CRISPRa in plants, we applied an engineering approach to systemically exploit different sgRNA scaffolds and transcription activators to develop the next-generation CRISPRa systems. We successfully developed CRISPR–Act3.0, which consists of dCas9–VP64, a gR2.0 scaffold with 2xMS2 stem loops, 10xGCN4 SunTag fused to RNA binding protein MCP and 2xTAD activators fused to scFv (Fig. 1a). We benchmarked CRISPR–Act3.0 as a third-generation CRISPRa system in plants as it outperformed all the second-generation CRISPRa systems in rice assays (Fig. 1d and Supplementary Fig. 3b)[11,13,16,17]. In CRISPR–Act3.0, multiple 2xTAD activators were recruited by the sgRNA scaffold through the MS2–MCP interaction. This feature may allow us to further develop complex CRISPRa systems with additional functionality through engineering orthogonal sgRNA scaffolds[8].

To make the CRISPR–Act3.0 systems user-friendly, we developed an efficient toolbox for multiplexed sgRNA assembly of up to six gRNA2.0 cassettes in one step based on PCR-free modular Golden Gate cloning and Gateway cloning systems[9,17,30,51] (Fig. 2a and Supplementary Fig. 4). We demonstrated that CRISPR–Act3.0 coupled with the M-tRNA system enabled multiplexed gene activation with the simultaneous activation of several enzyme-encoding genes involved in the β-carotene pathway as well as in the proanthocyanidin pathway in rice (Fig. 2c–e and Supplementary Figs. 6–8), suggesting promising application of CRISPR–Act3.0 in plant metabolic engineering. We also demonstrated CRISPR–Act3.0 for the simultaneous modification of two independent traits (flowering and trichome development) through multiplexed gene activation in *Arabidopsis* (Fig. 3). Strikingly, the *Arabidopsis* plants with the *AtFT* activation nearly reduced the plant life cycle by half (for example, ~30 days) (Fig. 3d). The phenotypes of early flowering and reduced trichome numbers due to simultaneous gene activation were stably transmitted to the T3 generation (Fig. 3e,f). These results suggest that CRISPR–Act3.0 holds great promise to accelerate crop breeding. Furthermore, we showed potent activation of a morphogenic gene in rice, *OsBBM1*, with up to 300-fold activation (Fig. 5f and Supplementary Fig. 3b). Our demonstration will promote the future use of CRISPR–Act3.0 for activating endogenous morphogenic genes to promote genotype-independent plant regeneration, as opposed to using heterologous morphogenic gene expression systems[52–54]. While both dpcoCas9–Act3.0 and dzCas9–Act3.0 showed comparable activation potency, we observed that the dzCas9–Act3.0 system

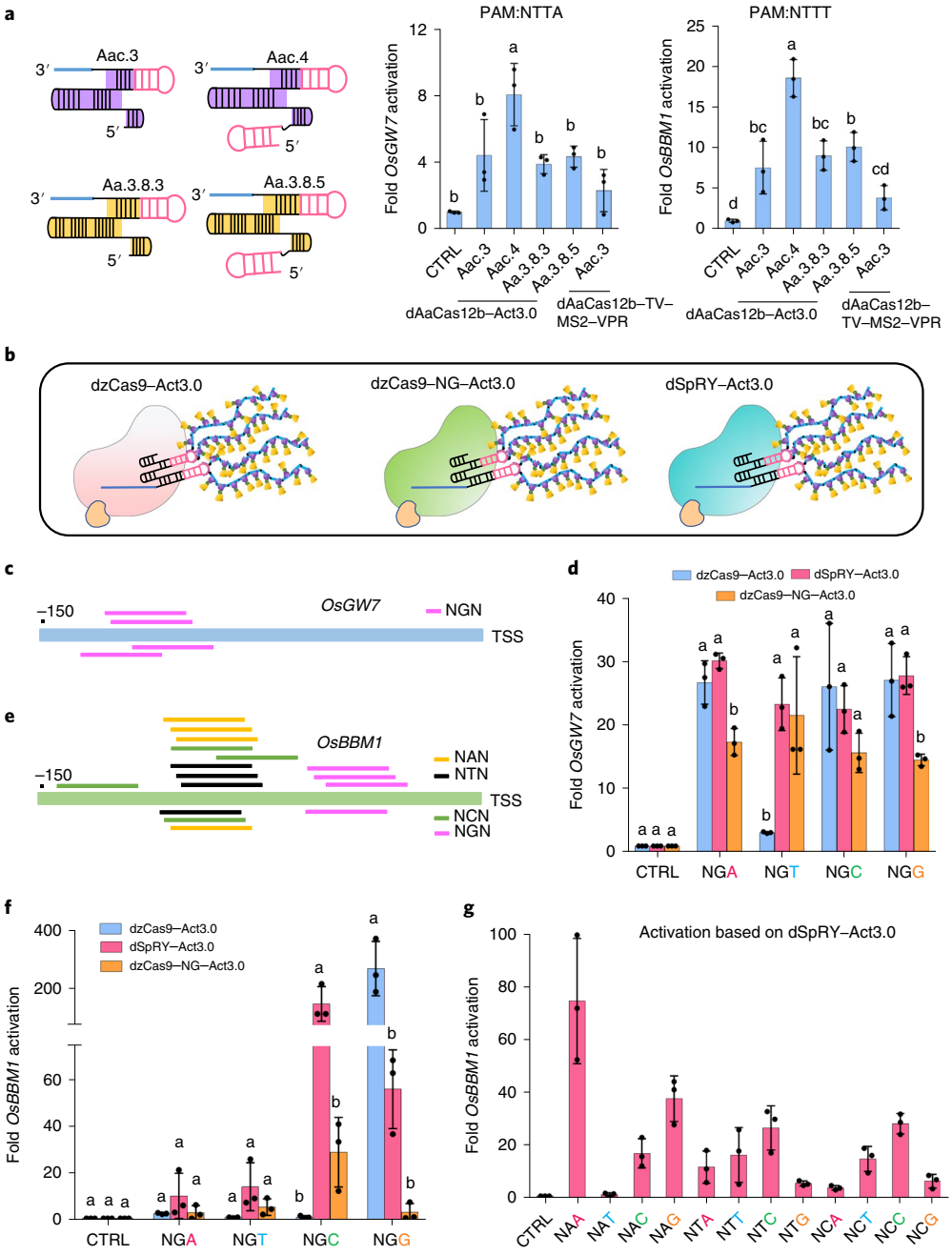

Fig. 5 | Expanding the targeting scope of CRISPR-Act3.0. a, Engineering and characterization of four dAaCas12b activation systems based on CRISPR-Act3.0 strategies. Left, schematics of four engineered Cas12b sgRNA scaffolds. The Aac.3 and Aa3.8.3 scaffolds each contain one MS2 RNA aptamer. The Aac.4 and Aa3.8.5 scaffolds each contain two MS2 RNA aptamers, as one MS2 was fused to the 5′ end of the sgRNA scaffold sequence. Right, RT-qPCR data showing the targeted activation of *OsGW7* and *OsBBM1* in rice protoplast cells. A total of five dAaCas12b activation systems are tested; among them, the combination of dAaCas12b-TV-MS2-VPR and Aac.3 sgRNA represents a potent activation system established recently[41]. **b**, Schematic illustrations of the engineered dzCas9-Act3.0, dzCas9-NG-Act3.0 and dSpRY-Act3.0 activation systems. **c**,**e**, Diagrams of the target site positions of *OsGW7* (**c**) and *OsBBM1* (**e**) for activation. The sgRNAs shown above the diagrams target the coding strand. The sgRNAs shown below the diagrams target the noncoding strand. **d**,**f**, Comparison of dzCas9-Act3.0, dzCas9-NG-Act3.0 and dSpRY-Act3.0-mediated *OsGW7* (**d**) and *OsBBM1* (**f**) activation at NGN PAMs. **g**, Comparison of dSpRY-Act3.0-mediated *OsBBM1* activation at NAN, NTN and NCN PAMs. For the RT-qPCR assays (**a**,**d**,**f**,**g**), T-DNA vectors without sgRNAs served as the negative control. *OsTubulin* is used as the endogenous control gene. All data are presented as the mean ± s.d. ($n = 3$ independent experiments). The different letters indicate significantly different mean values at $P < 0.05$ (one-way ANOVA with post-hoc Tukey test).

is more robust, as it does not cause plasmid DNA recombination when combined with M-tRNA or M-U3 sgRNAs and expressed in *A. tumefaciens* strains (Supplementary Fig. 10). We therefore recommend that researchers use dzCas9–Act3.0 for plant gene activation in their studies.

Previous studies have demonstrated that CRISPRa potency is highly sensitive to sgRNA target position relative to the TSS[23,29,55]. The optimal targeting window for CRISPRa in mammalian cells, bacteria and plants has been reported to be the 200 bp, 60–90 bp and 350 bp upstream region of the TSS[23,29,55]. However, only limited

sgRNAs and a few genes were tested in these studies[23,29,55]. By analysing activation data from 16 genes with 56 sgRNAs, we identified the 0-bp to −200-bp region from the TSS as a high-activity window for CRISPR–Act3.0-based gene activation in plants (Fig. 4a), which is similar to that of the dCas9–TV system[13,29]. Interestingly, we found that sgRNAs targeting the noncoding strand of DNA and with balanced GC contents are more likely to result in high levels of gene activation (Fig. 4a,b). However, to ensure efficient activation, a prescreen step for the best sgRNAs using a cell-based assay is always recommended. These observations also suggest that it is important to broaden the targeting scope for the successful implementation of CRISPRa in plants.

Towards this end, we developed an improved dAaCas12b-based activation system for targeting VTTV PAMs[41] with a new engineered sgRNA scaffold, Aac.4 (Fig. 5a), although the activation potency was still not as strong as that of dCas9-based CRISPR–Act3.0. To further broaden the targeting scope of dCas9-based CRISPR–Act3.0, we developed dzCas9–NG–Act3.0 based on Cas9–NG[43] and dSpRY–Act3.0 based on SpRY[49]. Our data suggest that dSpRY–Act3.0 can achieve near-PAM-less gene activation, which worked well particularly at NGN and NAN PAMs (Fig. 5d–g). Consistently, three recent studies demonstrated that SpRY could be used in genome editing at all NNN PAMs and exhibited a preference for NGN and NAN PAMs in rice[56–58]. Notably, high-frequency SpRY-mediated T-DNA self-editing was observed. The T-DNA self-targeting property could have compromised the activation potency of dSpRY–Act3.0 in our rice protoplast assays, due to the high copy numbers of plasmids used. Consequently, dSpRY–Act3.0 may induce higher activation efficiency in stable plants, although this needs to be tested. Taken together, these results demonstrate the high flexibility and adaptability of the CRISPR–Act3.0 strategy, which can be efficiently adapted to other CRISPR–Cas systems. The development of the dAaCas12b–Act3.0 and dSpRY–Act3.0 systems greatly reduces the PAM restriction and provides users with high flexibility in choosing targeting sites.

In conclusion, we have developed a highly efficient CRISPR–Act3.0 toolbox for multiplexed gene activation in plants. This toolbox would aid many applications including rewiring metabolic pathways, investigating gene regulatory networks and conducting genome-wide screens for identifying key genes in regulating plant development and stress responses.

Methods

Construction of Golden Gate and Gateway compatible CRISPR–Act3.0 vectors. The details about the construction of Gateway modular vectors for CRISPR–Act3.0 and Golden Gate modular vectors for multiplexing sgRNAs are available in the Supplementary Methods. The sequences of activators used in this study are summarized in Supplementary Fig. 13. The gBlocks and oligonucleotides in this study are summarized in Supplementary Table 1.

Assembly of T-DNA expression vectors. The final T-DNA expression vectors were assembled by a Multisite Gateway cloning strategy with the attR1-attR2 destination vector pYPQ203 (Addgene no. 86207) for rice, pYPQ202 (Addgene no. 86198) for *Arabidopsis*, pCGS710 (a gift from C. Starker and D. Voytas from the University of Minnesota) for tomato, an attL1-attR5 Cas activator entry clone and an attL5-attL2 sgRNA expression entry clone using Gateway LR clonase II (Invitrogen). The detailed procedure is described in the Supplementary Methods.

Rice and tomato protoplast transformation. The *japonica* cultivar Kitaake, the *indica* cultivar Kasalath and the tomato cultivar M82 were used in this study for the protoplast transformation assays. Rice protoplast isolation and transformation were performed as described previously with minor modifications[41]. In the tomato protoplast assays, the protoplasts were isolated from cotyledons of eight-day-old tomato seedlings. The protoplast isolation and transformation followed the same protocol as for rice with minor modifications. The tomato protoplast cells were collected from enzyme solution, resuspended in 0.55 M sucrose (pH 5.7) and then carefully overlayed with 2 ml of W5 solution without mixing. Protoplast cells were collected from the interface of the sucrose and W5 solutions after centrifugation at 200 *g* for 30 min, washed with W5 solution, and finally resuspended in MMG solution. To detect mCherry signals, plasmid DNA (20 μg per construct) was introduced into 180 μl of rice protoplasts by PEG-mediated transfection. The transfected protoplasts were incubated at 32 °C in the dark for 24 h and then collected for detecting mCherry signals using a fluorescence microscope. To determine the expression levels of the targeted genes, plasmid DNA (40 μg per construct) was introduced into 360 μl of rice protoplasts (2×10^6 cells per ml) or tomato protoplasts (1×10^6 cells per ml) by PEG-mediated transfection. The transfected protoplasts were incubated at 32 °C (rice) or 25 °C (tomato) in the dark. At 48 h after transfection, the protoplasts were collected for RNA extraction.

Rice stable transformation. To obtain transgenic plants, the T-DNA constructs were transformed into the *A. tumefaciens* strain EHA105. The *Agrobacterium*-mediated transformation of callus cells of Kasalath was performed as previously reported[41]. The transgenic rice plants were grown in an environmental chamber at 29 °C under a 16-h-light/8-h-dark cycle.

***Arabidopsis* transformation.** The Columbia-0 (Col-0) ecotype of *Arabidopsis thaliana* was used in this study. To obtain transgenic lines, the T-DNA constructs were transformed into the *Agrobacterium* strain GV3101, which were then transformed into wild-type plants of *Arabidopsis* using the floral dip method[59]. Seeds for the T1 to T3 generations were sterilized using 50% bleach and 0.05% Tween, vernalized at 4 °C in the dark for 3 days and then plated on MS-hygromycin plates. After one week, the transgenic plants were transferred to hygromycin-free plates for a week of recovery before being moved to soil. Transgenic *Arabidopsis* plants were grown in a growth chamber at 22 °C under a 16-h-light/8-h-dark cycle and 60% relative humidity.

DNA extraction, RNA extraction and qPCR analysis. Leaf and callus tissues of transgenic rice were collected for DNA extraction using the CTAB method[60]. The CRISPR–Act3.0 components in the transgenic tissues were detected using PCR with four pairs of primers. Leaf and callus tissues of transgenic rice, whole transgenic *Arabidopsis* seedlings or approximately 1 to 5×10^5 rice or tomato protoplast cells were used for RNA extraction. Total RNA was extracted from protoplast cells using TRIzol reagent (Thermo Fisher Scientific) according to the manufacturer's instructions. DNA was first removed from the total RNA samples by treatment with DNase I (RNase-free) (New England Biolabs). Then, 500–1,000 ng of total RNA was used for cDNA synthesis using the SuperScript III First-Strand Synthesis Kit (Invitrogen). The qPCR analysis was performed using the AzuraQuant Green Fast qPCR Mix (Azura Genomics) coupled with the CFX96 Touch Real-Time PCR Detection System (Bio-Rad) to detect transcript expression levels. *OsTubulin*, *EF-1α* and *SlUbi3* were used as the endogenous control genes for rice, *Arabidopsis* and tomato, respectively, and fold changes were calculated by the $2^{-\Delta\Delta Ct}$ method. All primers used in this study are listed in Supplementary Table 1.

Reporting Summary. Further information on research design is available in the Nature Research Reporting Summary linked to this article.

Data availability

The 25 Golden Gate and Gateway compatible vectors for the CRISPR–Act3.0 systems are available from Addgene: pYPQ131–tRNA2.0 (no. 158393), pYPQ132–tRNA2.0 (no. 158394), pYPQ133–tRNA2.0 (no. 158395), pYPQ134–tRNA2.0 (no. 158396), pYPQ135–tRNA2.0 (no. 158397), pYPQ136–tRNA2.0 (no. 158398), pYPQ142–ZmUbi–tRNA (no. 158578), pYPQ143–ZmUbi–tRNA (no. 158400), pYPQ144–ZmUbi–tRNA (no. 158402), pYPQ145–ZmUbi–tRNA (no. 158403), pYPQ146–ZmUbi–tRNA (no. 158404), pYPQ141–ZmUbi–RZ–Aac.4 (no. 158406), pYPQ141–ZmUbi–RZ–Aa3.8.5 (no. 158407), pYPQ–dpcoCas9–Act3.0 (no. 158408), pYPQ–dpcoCas9–TV (no. 158409), pYPQ–dpcoCas9–SunTag (no. 158410), pYPQ–dpcoCas9–EV2.1 (no. 158411), pYPQ–dAaCas12b–Act3.0 (no. 158413), pYPQ–dzCas9–Act3.0 (no. 158414), pYPQ–dzCas9–NG–Act3.0 (no. 158415), pYPQ–dSpRY–Act3.0 (no. 158416), pYPQ134B2.0 (no. 167158), pYPQ135B2.0 (no. 167159), pYPQ136B2.0 (no. 167160) and pYPQ141D–gRNA2.1 (no. 167161).

Received: 27 July 2020; Accepted: 27 May 2021;
Published online: 24 June 2021

References

1. Voytas, D. F. Plant genome engineering with sequence-specific nucleases. *Annu. Rev. Plant Biol.* **64**, 327–350 (2013).
2. Zhang, Y., Malzahn, A. A., Sretenovic, S. & Qi, Y. The emerging and uncultivated potential of CRISPR technology in plant science. *Nat. Plants* **5**, 778–794 (2019).
3. Schindele, A., Dorn, A. & Puchta, H. CRISPR/Cas brings plant biology and breeding into the fast lane. *Curr. Opin. Biotechnol.* **61**, 7–14 (2020).
4. Chen, K., Wang, Y., Zhang, R., Zhang, H. & Gao, C. CRISPR/Cas genome editing and precision plant breeding in agriculture. *Annu. Rev. Plant Biol.* **70**, 667–697 (2019).
5. Maeder, M. L. et al. CRISPR RNA-guided activation of endogenous human genes. *Nat. Methods* **10**, 977–979 (2013).

6. Perez-Pinera, P. et al. RNA-guided gene activation by CRISPR–Cas9-based transcription factors. *Nat. Methods* **10**, 973–976 (2013).
7. Li, Z., Xiong, X. & Li, J. The working dead: repurposing inactive CRISPR-associated nucleases as programmable transcriptional regulators in plants. *aBIOTECH* **1**, 32–40 (2020).
8. Pan, C., Sretenovic, S. & Qi, Y. CRISPR/dCas-mediated transcriptional and epigenetic regulation in plants. *Curr. Opin. Plant Biol.* **60**, 101980 (2021).
9. Lowder, L. G. et al. A CRISPR/Cas9 toolbox for multiplexed plant genome editing and transcriptional regulation. *Plant Physiol.* **169**, 971–985 (2015).
10. Piatek, A. et al. RNA-guided transcriptional regulation in planta via synthetic dCas9-based transcription factors. *Plant Biotechnol. J.* **13**, 578–589 (2014).
11. Papikian, A., Liu, W., Gallego-Bartolome, J. & Jacobsen, S. E. Site-specific manipulation of *Arabidopsis* loci using CRISPR–Cas9 SunTag systems. *Nat. Commun.* **10**, 729 (2019).
12. Gilbert, L. A. et al. Genome-scale CRISPR-mediated control of gene repression and activation. *Cell* **159**, 647–661 (2014).
13. Li, Z. et al. A potent Cas9-derived gene activator for plant and mammalian cells. *Nat. Plants* **3**, 930–936 (2017).
14. Xiong, X., Liang, J., Li, Z., Gong, B. Q. & Li, J. F. Multiplex and optimization of dCas9–TV-mediated gene activation in plants. *J. Integr. Plant Biol.* **63**, 634–645 (2021).
15. Chavez, A. et al. Highly efficient Cas9-mediated transcriptional programming. *Nat. Methods* **12**, 326–328 (2015).
16. Selma, S. et al. Strong gene activation in plants with genome-wide specificity using a new orthogonal CRISPR/Cas9-based programmable transcriptional activator. *Plant Biotechnol. J.* **17**, 1703–1705 (2019).
17. Lowder, L. G. et al. Robust transcriptional activation in plants using multiplexed CRISPR–Act2.0 and mTALE–Act systems. *Mol. Plant* **11**, 245–256 (2018).
18. Ma, H. et al. CRISPR-Sirius: RNA scaffolds for signal amplification in genome imaging. *Nat. Methods* **15**, 928–931 (2018).
19. Qin, P. et al. Live cell imaging of low- and non-repetitive chromosome loci using CRISPR–Cas9. *Nat. Commun.* **8**, 14725 (2017).
20. Xie, K., Minkenberg, B. & Yang, Y. Boosting CRISPR/Cas9 multiplex editing capability with the endogenous tRNA-processing system. *Proc. Natl Acad. Sci. USA* **112**, 3570–3575 (2015).
21. Kamiyama, D. et al. Versatile protein tagging in cells with split fluorescent protein. *Nat. Commun.* **7**, 11046 (2016).
22. Li, J. F. et al. Multiplex and homologous recombination-mediated genome editing in *Arabidopsis* and *Nicotiana benthamiana* using guide RNA and Cas9. *Nat. Biotechnol.* **31**, 688–691 (2013).
23. Konermann, S. et al. Genome-scale transcriptional activation by an engineered CRISPR–Cas9 complex. *Nature* **517**, 583–588 (2015).
24. Khanday, I., Skinner, D., Yang, B., Mercier, R. & Sundaresan, V. A male-expressed rice embryogenic trigger redirected for asexual propagation through seeds. *Nature* **565**, 91–95 (2019).
25. Tang, X. et al. Single transcript unit CRISPR 2.0 systems for robust Cas9 and Cas12a mediated plant genome editing. *Plant Biotechnol. J.* https://doi.org/10.1111/pbi.13068 (2018).
26. Zhang, Y. et al. A gRNA–tRNA array for CRISPR–Cas9 based rapid multiplexed genome editing in *Saccharomyces cerevisiae*. *Nat. Commun.* **10**, 1053 (2019).
27. Port, F. & Bullock, S. L. Augmenting CRISPR applications in *Drosophila* with tRNA-flanked sgRNAs. *Nat. Methods* **13**, 852–854 (2016).
28. Dong, F., Xie, K., Chen, Y., Yang, Y. & Mao, Y. Polycistronic tRNA and CRISPR guide-RNA enables highly efficient multiplexed genome engineering in human cells. *Biochem. Biophys. Res. Commun.* **482**, 889–895 (2017).
29. Gong, X., Zhang, T., Xing, J., Wang, R. & Zhao, Y. Positional effects on efficiency of CRISPR/Cas9-based transcriptional activation in rice plants. *aBIOTECH* **1**, 1–5 (2020).
30. Malzahn, A., Zhang, Y. & Qi, Y. CRISPR–Act2.0: an improved multiplexed system for plant transcriptional activation. *Methods Mol. Biol.* **1917**, 83–93 (2019).
31. He, F., Pan, Q. H., Shi, Y. & Duan, C. Q. Biosynthesis and genetic regulation of proanthocyanidins in plants. *Molecules* **13**, 2674–2703 (2008).
32. Xing, H. L. et al. A CRISPR/Cas9 toolkit for multiplex genome editing in plants. *BMC Plant Biol.* **14**, 327 (2014).
33. Zhou, J. et al. Application and future perspective of CRISPR/Cas9 genome editing in fruit crops. *J. Integr. Plant Biol.* **62**, 269–286 (2020).
34. Wigge, P. A. et al. Integration of spatial and temporal information during floral induction in *Arabidopsis*. *Science* **309**, 1056–1059 (2005).
35. Wang, S. et al. TRICHOMELESS1 regulates trichome patterning by suppressing GLABRA1 in *Arabidopsis*. *Development* **134**, 3873–3882 (2007).
36. Turck, F., Fornara, F. & Coupland, G. Regulation and identity of florigen: FLOWERING LOCUS T moves center stage. *Annu. Rev. Plant Biol.* **59**, 573–594 (2008).
37. Klimek-Chodacka, M., Oleszkiewicz, T., Lowder, L. G., Qi, Y. & Baranski, R. Efficient CRISPR/Cas9-based genome editing in carrot cells. *Plant Cell Rep.* **37**, 575–586 (2018).
38. Lei, Y. et al. CRISPR-P: a web tool for synthetic single-guide RNA design of CRISPR-system in plants. *Mol. Plant* **7**, 1494–1496 (2014).
39. Jinek, M. et al. A programmable dual-RNA-guided DNA endonuclease in adaptive bacterial immunity. *Science* **337**, 816–821 (2012).
40. Das, S. & Bansal, M. Variation of gene expression in plants is influenced by gene architecture and structural properties of promoters. *PLoS ONE* **14**, e0212678 (2019).
41. Ming, M. et al. CRISPR–Cas12b enables efficient plant genome engineering. *Nat. Plants* **6**, 202–208 (2020).
42. Teng, F. et al. Repurposing CRISPR–Cas12b for mammalian genome engineering. *Cell Discov.* **4**, 63 (2018).
43. Nishimasu, H. et al. Engineered CRISPR–Cas9 nuclease with expanded targeting space. *Science* **361**, 1259–1262 (2018).
44. Endo, M. et al. Genome editing in plants by engineered CRISPR–Cas9 recognizing NG PAM. *Nat. Plants* **5**, 14–17 (2019).
45. Ren, B. et al. Cas9-NG greatly expands the targeting scope of the genome-editing toolkit by recognizing NG and other atypical PAMs in rice. *Mol. Plant* **12**, 1015–1026 (2019).
46. Zhong, Z. et al. Improving plant genome editing with high-fidelity xCas9 and non-canonical PAM-targeting Cas9-NG. *Mol. Plant* https://doi.org/10.1016/j.molp.2019.03.011 (2019).
47. Hua, K., Tao, X., Han, P., Wang, R. & Zhu, J. K. Genome engineering in rice using Cas9 variants that recognize NG PAM sequences. *Mol. Plant* **12**, 1003–1014 (2019).
48. Ge, Z. et al. Engineered xCas9 and SpCas9-NG variants broaden PAM recognition sites to generate mutations in *Arabidopsis* plants. *Plant Biotechnol. J.* **17**, 1865–1867 (2019).
49. Walton, R. T., Christie, K. A., Whittaker, M. N. & Kleinstiver, B. P. Unconstrained genome targeting with near-PAMless engineered CRISPR–Cas9 variants. *Science* https://doi.org/10.1126/science.aba8853 (2020).
50. Zhang, Y. et al. Comparison of non-canonical PAMs for CRISPR/Cas9-mediated DNA cleavage in human cells. *Sci. Rep.* **4**, 5405 (2014).
51. Lowder, L. G., Paul, J. W. III & Qi, Y. Multiplexed transcriptional activation or repression in plants using CRISPR–dCas9 based systems. *Methods Mol. Biol.* **1629**, 167–184 (2017).
52. Lowe, K. et al. Morphogenic regulators *Baby boom* and *Wuschel* improve monocot transformation. *Plant Cell* https://doi.org/10.1105/tpc.16.00124 (2016).
53. Mookkan, M., Nelson-Vasilchik, K., Hague, J., Zhang, Z. J. & Kausch, A. P. Selectable marker independent transformation of recalcitrant maize inbred B73 and sorghum P898012 mediated by morphogenic regulators BABY BOOM and WUSCHEL2. *Plant Cell Rep.* **36**, 1477–1491 (2017).
54. Maher, M. F. et al. Plant gene editing through de novo induction of meristems. *Nat. Biotechnol.* **38**, 84–89 (2020).
55. Dong, C., Fontana, J., Patel, A., Carothers, J. M. & Zalatan, J. G. Synthetic CRISPR–Cas gene activators for transcriptional reprogramming in bacteria. *Nat. Commun.* **9**, 2489 (2018).
56. Ren, Q. et al. PAM-less plant genome editing using a CRISPR–SpRY toolbox. *Nat. Plants* **7**, 25–33 (2021).
57. Xu, Z. et al. SpRY greatly expands the genome editing scope in rice with highly flexible PAM recognition. *Genome Biol.* **22**, 6 (2021).
58. Li, J. et al. Genome editing mediated by SpCas9 variants with broad non-canonical PAM compatibility in plants. *Mol. Plant* **14**, 352–360 (2021).
59. Clough, S. J. & Bent, A. F. Floral dip: a simplified method for *Agrobacterium*-mediated transformation of *Arabidopsis thaliana*. *Plant J.* **16**, 735–743 (1998).
60. Stewart, C. N. Jr. & Via, L. E. A rapid CTAB DNA isolation technique useful for RAPD fingerprinting and other PCR applications. *Biotechniques* **14**, 748–750 (1993).

Acknowledgements

This work was supported by University of Maryland start-up funds, the National Science Foundation Plant Genome Research Program grants (award nos. IOS-1758745 and IOS-2029889), Biotechnology Risk Assessment Grant Program competitive grants (award nos. 2018-33522-28789 and 2020-33522-32274) from the US Department of Agriculture, a Foundation for Food and Agriculture Research grant (award no. 593603) and Syngenta. A.A.M. was supported by an NRT-INFEWS: UMD Global STEWARDS (STEM Training at the Nexus of Energy, Water Reuse and Food Systems) award to the University of Maryland School of Public Health from the National Science Foundation National Research Traineeship Program (award no. 1828910). The content of this publication is solely the responsibility of the authors and does not necessarily represent the official views of these funding agencies.

Author contributions

Y.Q. and C.P. designed the experiments. C.P., X.W., N.K., Y.Z. and S.S. generated all the constructs. C.P., X.W. and Y.C. performed the transient assays in protoplasts. C.P.

generated the stable transgenic rice and analysed the plants. C.P. and A.A.M. generated the stable transgenic *Arabidopsis* plants. C.P. and X.W. conducted the transcriptional activation assays. K.M. and P.M.S. helped with the design of metabolic pathway gene activation. Y.Q. and C.P. wrote the paper with input from the other authors. All authors read and approved the final manuscript.

Competing interests

Y.Q. and C.P. are inventors on a US Provisional Patent Application (no. 63066674) that has been filed on the CRISPR–Act3.0 system in this study. All other authors declare no competing interests.

Additional information

Supplementary information The online version contains supplementary material available at https://doi.org/10.1038/s41477-021-00953-7.

Correspondence and requests for materials should be addressed to Y.Q.

Peer review information *Nature Plants* thanks Jian-feng Li and the other, anonymous, reviewer(s) for their contribution to the peer review of this work.

Reprints and permissions information is available at www.nature.com/reprints.

Publisher's note Springer Nature remains neutral with regard to jurisdictional claims in published maps and institutional affiliations.

nature research

Corresponding author(s): Yiping Qi

Last updated by author(s): 05/22/2021

Reporting Summary

Nature Research wishes to improve the reproducibility of the work that we publish. This form provides structure for consistency and transparency in reporting. For further information on Nature Research policies, see Authors & Referees and the Editorial Policy Checklist.

Statistics

For all statistical analyses, confirm that the following items are present in the figure legend, table legend, main text, or Methods section.

n/a	Confirmed	
☐	☒	The exact sample size (*n*) for each experimental group/condition, given as a discrete number and unit of measurement
☐	☒	A statement on whether measurements were taken from distinct samples or whether the same sample was measured repeatedly
☐	☒	The statistical test(s) used AND whether they are one- or two-sided *Only common tests should be described solely by name; describe more complex techniques in the Methods section.*
☒	☐	A description of all covariates tested
☒	☐	A description of any assumptions or corrections, such as tests of normality and adjustment for multiple comparisons
☐	☒	A full description of the statistical parameters including central tendency (e.g. means) or other basic estimates (e.g. regression coefficient) AND variation (e.g. standard deviation) or associated estimates of uncertainty (e.g. confidence intervals)
☐	☒	For null hypothesis testing, the test statistic (e.g. *F*, *t*, *r*) with confidence intervals, effect sizes, degrees of freedom and *P* value noted *Give P values as exact values whenever suitable.*
☒	☐	For Bayesian analysis, information on the choice of priors and Markov chain Monte Carlo settings
☒	☐	For hierarchical and complex designs, identification of the appropriate level for tests and full reporting of outcomes
☒	☐	Estimates of effect sizes (e.g. Cohen's *d*, Pearson's *r*), indicating how they were calculated

Our web collection on statistics for biologists contains articles on many of the points above.

Software and code

Policy information about availability of computer code

Data collection	None used
Data analysis	SnapGene 4.3.11 was used to analyze and construct DNA vectors. BioRad CFX Manager and excel were used to analyze qRT-PCR data. Promoter sequences were obtained from Phytozome v12.1 (https://phytozome.jgi.doe.gov/pz/portal.html). Multiple DNA sequence alignment was performed using the Clustal Omega (https://www.ebi.ac.uk/Tools/msa/clustalo/).

For manuscripts utilizing custom algorithms or software that are central to the research but not yet described in published literature, software must be made available to editors/reviewers. We strongly encourage code deposition in a community repository (e.g. GitHub). See the Nature Research guidelines for submitting code & software for further information.

Data

Policy information about availability of data

All manuscripts must include a data availability statement. This statement should provide the following information, where applicable:

- Accession codes, unique identifiers, or web links for publicly available datasets
- A list of figures that have associated raw data
- A description of any restrictions on data availability

All generated and analysed data from this study are included in the published article and its Supplementary Information. All 25 CRISPR-Act3.0 Gateway entry clones for plant genome engineering have submitted to Addgene for public dissemination.

Field-specific reporting

Please select the one below that is the best fit for your research. If you are not sure, read the appropriate sections before making your selection.

☒ Life sciences ☐ Behavioural & social sciences ☐ Ecological, evolutionary & environmental sciences

For a reference copy of the document with all sections, see nature.com/documents/nr-reporting-summary-flat.pdf

Life sciences study design

All studies must disclose on these points even when the disclosure is negative.

Sample size	For rice and tomato protoplast assays, 360 µL rice protoplasts (2x1,000,000 cells/mL) or tomato protoplasts (1x1,000,000 cells/mL) were used for PEG-mediated transfection per sample. The cell counting was performed using the disposable hemocytometer DHC-N01 with a microscope. For stable transformation, 12 individual transgenic lines were evaluated in the rice T0 generation and Arabidopsis T1 generation, respectively, and about 70 individual transgenic plants were evaluated in T2 and T3 generation of Arabidopsis plants.
Data exclusions	No data was excluded.
Replication	For rice and tomato protoplast assays, three biological replicates were used for generating most of the data. Two biological replicates were used for two supplementary figures. For prescreening individual sgRNAs for gene activation, one biological replicate with three technical replicates was performed. For stable transformation of each construct, 12 or more individual lines and three technical replicates was performed.
Randomization	In experiments involving genotypes, seedlings were randomly grown on the petri-dishes or in the trays. The sgRNAs used in this study were randomly designed and picked for assessment in the experiments.
Blinding	Blinding was not relevant to this study since the data were always collected according to the designated plasmids and genotypes of the plants.

Reporting for specific materials, systems and methods

We require information from authors about some types of materials, experimental systems and methods used in many studies. Here, indicate whether each material, system or method listed is relevant to your study. If you are not sure if a list item applies to your research, read the appropriate section before selecting a response.

Materials & experimental systems

n/a	Involved in the study
☒	☐ Antibodies
☒	☐ Eukaryotic cell lines
☒	☐ Palaeontology
☒	☐ Animals and other organisms
☒	☐ Human research participants
☒	☐ Clinical data

Methods

n/a	Involved in the study
☒	☐ ChIP-seq
☒	☐ Flow cytometry
☒	☐ MRI-based neuroimaging